Title

PCB 95 promotes dendritic growth in primary rat hippocampal neurons via mTOR-dependent mechanisms

Journal

Archives of Toxicology, 92(10)

ISSN

0340-5761

Authors

Keil, Kimberly P

Miller, Galen W

Chen, Hao

et al.

Publication Date

2018-10-01

DOI

10.1007/s00204-018-2285-x

Peer reviewed

Archives of Toxicology (2018) 92:3163–3173
https://doi.org/10.1007/s00204-018-2285-x

ORGAN TOXICITY AND MECHANISMS

PCB 95 promotes dendritic growth in primary rat hippocampal neurons via mTOR-dependent mechanisms

Kimberly P. Keil[1] · Galen W. Miller[1,2] · Hao Chen[1] · Sunjay Sethi[1] · Martin R. Schmuck[1] · Kiran Dhakal[1,3] · Ji Won Kim[1] · Pamela J. Lein[1]

Received: 6 June 2018 / Accepted: 6 August 2018 / Published online: 21 August 2018

Abstract

Polychlorinated biphenyls (PCBs), and in particular non-dioxin-like (NDL) congeners, continue to pose a significant risk to the developing nervous system. PCB 95, a prevalent NDL congener in the human chemosphere, promotes dendritic growth in rodent primary neurons by activating calcium-dependent transcriptional mechanisms that normally function to link activity to dendritic growth. Activity-dependent dendritic growth is also mediated by calcium-dependent translational mechanisms involving mechanistic target of rapamycin (mTOR), suggesting that the dendrite-promoting activity of PCB 95 may also involve mTOR signaling. Here, we test this hypothesis using primary neuron-glia co-cultures derived from the hippocampi of postnatal day 0 Sprague Dawley rats. PCB 95 (1 nM) activated mTOR in hippocampal cultures as evidenced by increased phosphorylation of mTOR at ser2448. Pharmacologic inhibition of mTOR signaling using rapamycin (20 nM), FK506 (5 nM), or 4EGI-1 (1 μM), and siRNA knockdown of mTOR, or the mTOR complex binding proteins, raptor or rictor, blocked PCB 95-induced dendritic growth. These data identify mTOR activation as a novel molecular mechanism contributing to the effects of PCB 95 on dendritic arborization. In light of clinical data linking gain-of-function mutations in mTOR signaling to neurodevelopmental disorders, our findings suggest that mTOR signaling may represent a convergence point for gene by environment interactions that confer risk for adverse neurodevelopmental outcomes.

Keywords Developmental neurotoxicity · Neurodevelopmental disorders · Persistent organic pollutants · Sholl analysis

Introduction

There is credible evidence that environmental factors influence risk of neurodevelopmental disorders (NDDs), particularly in genetically susceptible individuals (Heyer and Meredith 2017; Lyall et al. 2017a). However, the identification of environmental factors that influence NDD risk and the mechanisms by which they interact with genetic susceptibilities to influence NDD risk are largely unknown. Polychlorinated biphenyls (PCBs) have been implicated as NDD risk factors (Landrigan et al. 2012; Stamou et al. 2013), and despite being banned from production since the late 1970s, PCBs remain persistent environmental toxicants with documented widespread exposure of pregnant women and young children (Herrick et al. 2007; Koh et al. 2016; Marek et al. 2017). Perinatal exposure to PCBs is associated with neuropsychological deficits in children (Berghuis et al. 2015; Lyall et al. 2017b), and confirmed in preclinical models (Sable and Schantz 2006; Ulbrich and Stahlmann 2004).

Preclinical studies demonstrate that developmental exposures to Aroclor 1254 or to the NDL congener, PCB 95, enhance dendritic growth and alter dendritic plasticity in the developing brain coincident with deficits in spatial learning and memory (Wayman et al. 2012b; Yang et al. 2009). In primary hippocampal neurons, PCB 95 promotes dendritic

Kimberly P. Keil and Galen W. Miller contributed equally to this manuscript.

Electronic supplementary material The online version of this article (https://doi.org/10.1007/s00204-018-2285-x) contains supplementary material, which is available to authorized users.

✉ Pamela J. Lein
pjlein@ucdavis.edu

[1] Department of Molecular Biosciences, School of Veterinary Medicine, University of California, Davis, 1089 Veterinary Medicine Drive, Davis, CA 95616, USA

[2] Present Address: BioPlx Microbiomics, Boulder, CO, USA

[3] Present Address: Laboratory Corporation of America (LabCorp), Research Triangle Park, NC, USA

growth via sensitization of ryanodine receptors (RyR) to release Ca^{2+} from intracellular stores, which triggers Ca^{2+}-dependent signaling pathways that activate transcriptional mechanisms of dendritic growth and spine formation (Lesiak et al. 2014; Wayman et al. 2012a). These effects phenocopy NDDs, which are also associated with enhanced dendritic arborization (Copf 2016) and with mutations in genes that encode signaling molecules important in activity-dependent dendritic growth (Ebert and Greenberg 2013; Stamou et al. 2013).

Activity-dependent dendritic growth is modulated not only by Ca^{2+}-dependent transcriptional mechanisms (Pessah et al. 2010; Wayman et al. 2012a), but also by Ca^{2+}-dependent translational mechanisms mediated largely by mTOR signaling (Kindler and Kreienkamp 2012; Sosanya et al. 2015). When activated, mTOR complex 1 (mTORC1), which includes mTOR, FK506-binding protein 12 (FKBP12), and the regulatory-associated protein of mTOR (raptor), phosphorylates 4EBP1/2, releasing eIF4E to bind eIF4GII, which initiates cap-dependent translation (Zhou and Huang 2010). In contrast, mTOR complex 2 (mTORC2), which is comprised of mTOR and the rapamycin-insensitive companion of mTOR (rictor), phosphorylates Akt (protein kinase B), and is linked to cell autophagy and cytoskeleton regulation. mTOR activation increases dendritic outgrowth and synaptogenesis (Urbanska et al. 2012), and mutations in both mTOR signaling pathways have been linked to increased risk for NDDs (Gipson and Johnston 2012; Switon et al. 2017; Troca-Marin et al. 2012; Wang and Doering 2013). Collectively, these observations suggest that mTOR signaling may contribute to PCB 95-induced dendritic growth. Here, we test this hypothesis in primary rat hippocampal neurons.

Materials and methods

Materials

PCB 95 (2,2′,3,5′,6-pentachlorobiphenyl) was purchased from AccuStandard, (Lot #010610KS, 99.7% pure, New Haven, CT). All PCB 95 stock solutions were made in dry sterile dimethylsulfoxide (DMSO, Sigma-Aldrich, St. Louis, MO). Plasmids encoding microtubule-associated-protein-2B (MAP2B)-pCAG-fusion protein red (FusRed) or MAP2B fused to enhanced green fluorescent protein (MAP2B-pCAG-EGFP) were generously provided by Dr. Gary Wayman (University of Washington, Pullman, WA) and have been previously characterized (Wayman et al. 2006). Predesigned Ambion Silencer Select siRNAs targeting mTOR (s132719), raptor (s143003), rictor (s160195), or scrambled siRNA (#4390844) were purchased from Thermo Fisher Scientific (Waltham, MA). FK506 was purchased from Cayman Chemical (Ann Arbor, MI); 4EGI-1, from Tocris (Minneapolis, MN); and rapamycin, from Selleckchem (Houston, TX).

Animals

All procedures involving animals were conducted in accordance with the NIH Guide for the Care and Use of Laboratory Animals and were approved by the University of California, Davis Institutional Animal Care and Use Committee. Timed-pregnant Sprague Dawley rats were purchased from Charles River Laboratory (Hollister, CA). All animals were housed in clear plastic shoebox cages containing corn cob bedding under constant temperature (22 ± 2 °C) and a 12 h light–dark cycle. Food and water were provided ad libitum.

Cell culture

Primary hippocampal cell cultures were prepared from postnatal day (P) 0—P1 rat pups with hippocampi from both sexes pooled as described previously (Wayman et al. 2006). Dissociated hippocampal cells were plated at a density of 83,000 cells/cm^2 on glass coverslips (Bellco Glass, Vineland, NJ) precoated with poly-L-lysine (0.5 mg/mL, Sigma-Aldrich) and maintained at 37 °C in NeuralQ Basal Medium supplemented with 2% GS21 (MTI-GlobalStem, Gaithersburg, MD) and 1% GlutaMAX (Thermo Fisher Scientific) under 5% CO_2. On day in vitro (DIV) 4, cultures were treated with cytosine β-D-arabinofuranoside hydrochloride (2.5 µM, Sigma-Aldrich) to limit glia cell proliferation. On DIV 6, cells were transfected with either MAP2B-pCAG-FusRed or MAP2B-pCAG-EGFP plasmids using Lipofectamine-2000 (Invitrogen, Carlsbad, CA) per the manufacturer's instructions. A subset of cultures was co-transfected with 1 nM predesigned Ambion Silencer Select siRNAs. On DIV 7, cells were treated with one or more of the following: vehicle (DMSO; $\leq 0.2\%$), PCB 95 (1 nM), FK506 (5 nM), or 4EGI (1 µM) diluted from 1,000x stocks directly into culture medium. Rapamycin (20 nM) was added on DIV 6 to pretreat cultures for 24 h prior to addition of vehicle or PCB 95 on DIV 7.

Immunocytochemistry

Cultures were fixed on DIV 9 with 4% paraformaldehyde (PFA, Sigma–Aldrich) for 20 min, and then permeabilized and immunostained as previously described (Chen et al. 2017). Primary antibodies included rabbit anti-mTOR (1:200, #2983, Cell Signaling, Danvers, MA), mouse anti-FKBP12 (1:100, sc-133067, Santa Cruz, Dallas, TX), and mouse anti RyR1/RyR2 (1:50, 34C, Developmental Studies Hybridoma Bank, Iowa City, IA). Secondary antibodies were purchased from Thermo Fisher Scientific and

included goat anti-rabbit Alexa 568 IgG (1:500, A-11036), goat anti-rabbit Alexa 647 IgG H + L (1:500, A-21244), goat anti-mouse IgG2a Alexa 647 (1:500, A-21241), and goat anti-mouse IgG1 Alexa 568 (1:500, A-21124). Negative controls were reacted with secondary antibodies only. Images were acquired on a Nikon N-SIM using broad-band diffraction grating (405,488,561,640 nm) with a 100x NA 1.49 objective. Images were acquired in Nikon "3D-SIM" mode (three diffraction grating angles, five translations), which cuts ~ 350 nm optical section using interference patterns between − 1, + 1, and 0 order diffraction lines (Gustafsson et al. 2008). Images were processed using the Nikon Elements SIM software control module (reconstructed image pixel size = 0.032 µm). Image planes were further preprocessed in Fiji (Schindelin et al. 2012) utilizing the rolling ball method (radius10) prior to being imported into Imaris8.2 (Bitplane) (x, y = 0.0313 µm, z = 0.133 µm) to generate movies (see Supplementary material).

Phosphorylated mTOR ELISA

On DIV 7, cultures were exposed for 2 h to one or more of the following: vehicle (DMSO; ≤ 0.2%), PCB 95 (1 nM), and/or rapamycin (20 nM). Cultures were pretreated with rapamycin (20 nM) for 24 h prior to the addition of vehicle or PCB 95. A PathScan Phospho-mTOR (Ser2448) Sandwich ELISA Kit (#7976C, Cell Signaling Technology) was used per the manufacturer's instructions to detect phosphorylated mTOR in cell lysates. Protein concentration was determined using Pierce BCA Kit (Thermo Fisher Scientific). Absorbance was read at 450 nm using a Synergy H1 Reader (Biotek Instruments, Winooski, VT). Average absorbance values from two technical replicates were normalized to untreated control wells within a dissection. Results are reported as mean ± SEM fold change from untreated control from n = 4 independent dissections.

Morphometric analysis

On DIV 9, cells were fixed with 4% PFA and mounted to glass slides using ProLong Gold antifade reagent with DAPI (Thermo Fisher Scientific). Images of EGFP or FusRed positive neurons were captured using an ImageExpressXL high-content imaging system (Molecular Devices, Sunnyvale, CA) with automated image acquisition software (Metaxpress Version 5.3.0.5, Molecular Devices). Neurons were chosen for morphological analyses using previously described criteria (Keil et al. 2017). The dendritic morphology of individual neurons was quantified by an individual blinded to experimental conditions using ImageJ software (Schneider et al. 2012) with the Sholl analysis plug-in v3.4.2 (Ferreira et al. 2014). Dendritic morphology was measured in neurons from three coverslips per group per dissection, using cultures prepared from at least three independent dissections. Data used to generate figures include neurons from at least 2–3 independent dissections.

Statistics

Data were tested for normality using Kolmogorov–Smirnov, D'Agostino and Pearson omnibus, and Shapiro–Wilk normality tests and Bartlett's test for equal variance using GraphPad Prism v 6.07 (San Diego, CA). Differences between two groups were assessed using Student's T test or Student's T Test with Welch's correction for parametric data and by the Mann–Whitney U test for nonparametric data. Differences between three or more groups were assessed using a one-way analysis of variance (ANOVA) with p set at 0.05 followed by Tukey's multiple comparison test for parametric data or Kruskal–Wallis test with Dunn's multiple comparison test for nonparametric data. Values for the area under the curve, distance from soma of peak intersection (peak X), and maximum dendritic intersections (peak Y) were calculated from Sholl profiles using the built in area under the curve analysis in GraphPad Prism Software. All results are reported as mean ± SEM.

Results

Primary hippocampal neuron-glia co-cultures express mTOR, FKBP12, and RyR1/2

The co-localization of mTOR, FKBP12, and RyR1/2 in primary hippocampal neurons was confirmed using structured illumination microscopy (SIM). Immunoreactivity for mTOR, RyR1/2 and FKBP12 was observed in close physical proximity in the soma and dendrites of DIV 9 hippocampal neurons (Fig. 1 and Supplemental movies 1, 2). mTOR was primarily localized surrounding the nucleus, while FKBP12 was present in both the perinuclear space as well as the nucleus (Fig. 1a). Both mTOR and FKBP12 were also present in distal dendrites (Fig. 1b). RyR1/2 displayed distinct punctuate staining surrounding the nucleus and was present in distal dendrites (Fig. 1c, d). RyR1/2 and mTOR immunoreactivity was present in MAP2B immunopositive processes (Fig. 1e, f).

PCB 95 promotes dendritic growth via mTOR activation

To determine whether PCB 95 activates mTOR at a concentration (1 nM) that promotes dendritic growth (Wayman et al. 2012a), we used a sandwich ELISA to quantify mTOR phosphorylated on Ser2448. Phosphorylated mTOR was significantly increased in DIV 7 hippocampal cultures exposed

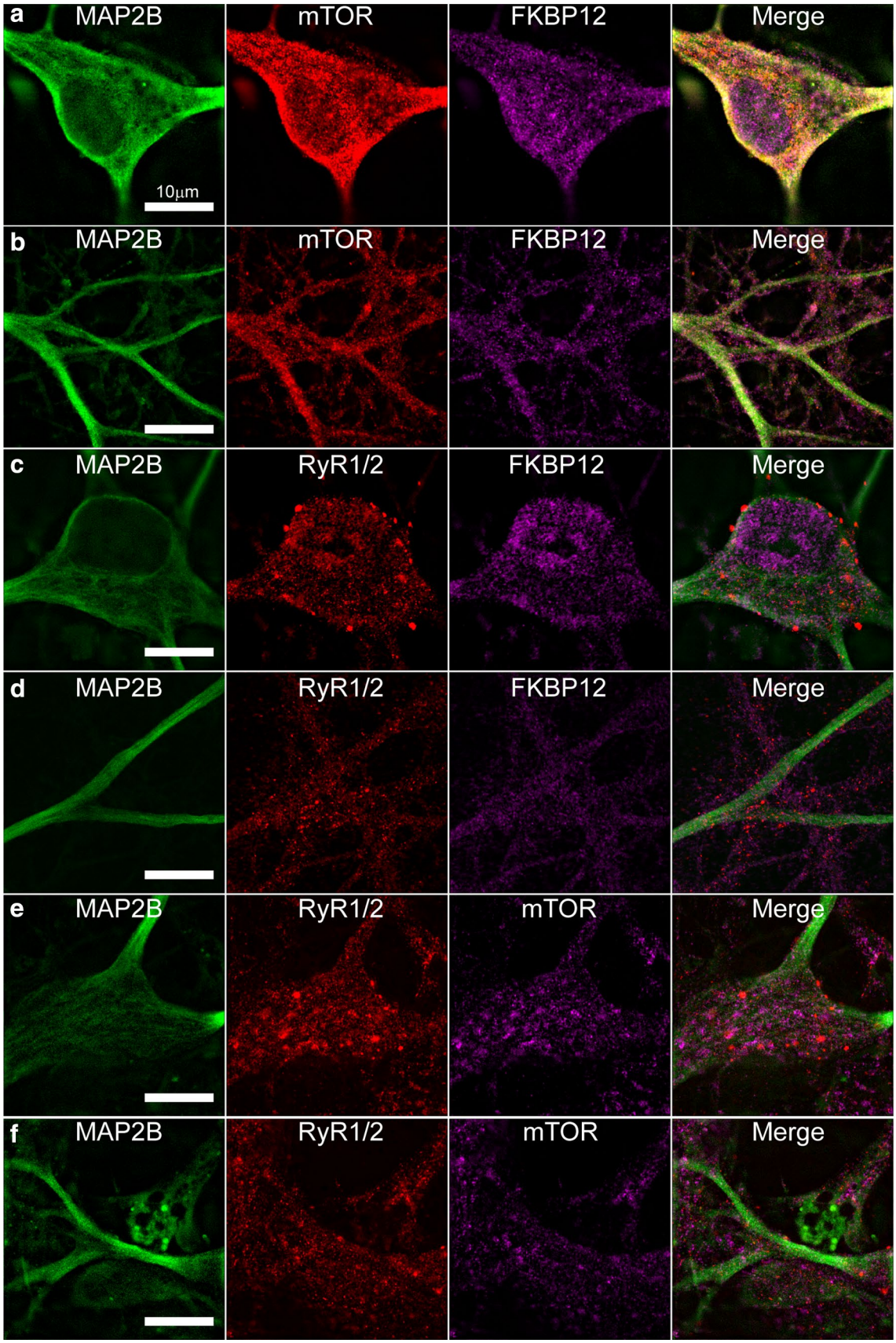
a
MAP2B
mTOR
FKBP12
Merge
10μm
b
MAP2B
mTOR
FKBP12
Merge
c
MAP2B
RyR1/2
FKBP12
Merge
d
MAP2B
RyR1/2
FKBP12
Merge
e
MAP2B
RyR1/2
mTOR
Merge
f
MAP2B
RyR1/2
mTOR
Merge

◂**Fig. 1** Representative SIM photomicrographs of the cell soma (**a, c, e**) and distal dendrites (**b, d, f**) of primary rat hippocampal neurons at 9 DIV transfected with MAP2B-EGFP and co-labeled with antibodies specific for **a, b** mTOR and FKBP12; **c, d** RyR1/2 and FKBP12; or **e, f** RyR1/2 and mTOR. Bar = 10 µm

to PCB 95 (1 nM) for 2 h relative to vehicle control cultures (Fig. 2b). PCB 95-induced phosphorylation of mTOR activation was blocked by the mTOR inhibitor, rapamycin (Fig. 2b).

To determine whether mTOR activation is causally linked to PCB 95-induced dendritic growth, we quantified dendritic growth in PCB-exposed cultures treated with pharmacologic agents that block mTOR signaling by interfering with mTOR interactions with FKBP12 (Fig. 2a). As determined by Sholl analysis, rapamycin blocked PCB 95-induced dendritic growth (Fig. 2c–f). Notably, rapamycin did not alter dendritic growth in vehicle control cultures (Fig. 2). To confirm the rapamycin observations, we used a different pharmacological inhibitor of the mTOR pathway, FK506, which acts to disrupt the interaction between FKBP12 and the mTOR complex (Schreiber et al. 2015). While FK506 had no effect on dendritic growth in vehicle control cultures, it significantly inhibited PCB 95-induced dendritic growth (Fig. 3).

To corroborate findings obtained using pharmacologic inhibition of mTOR signaling, we assessed the effects of

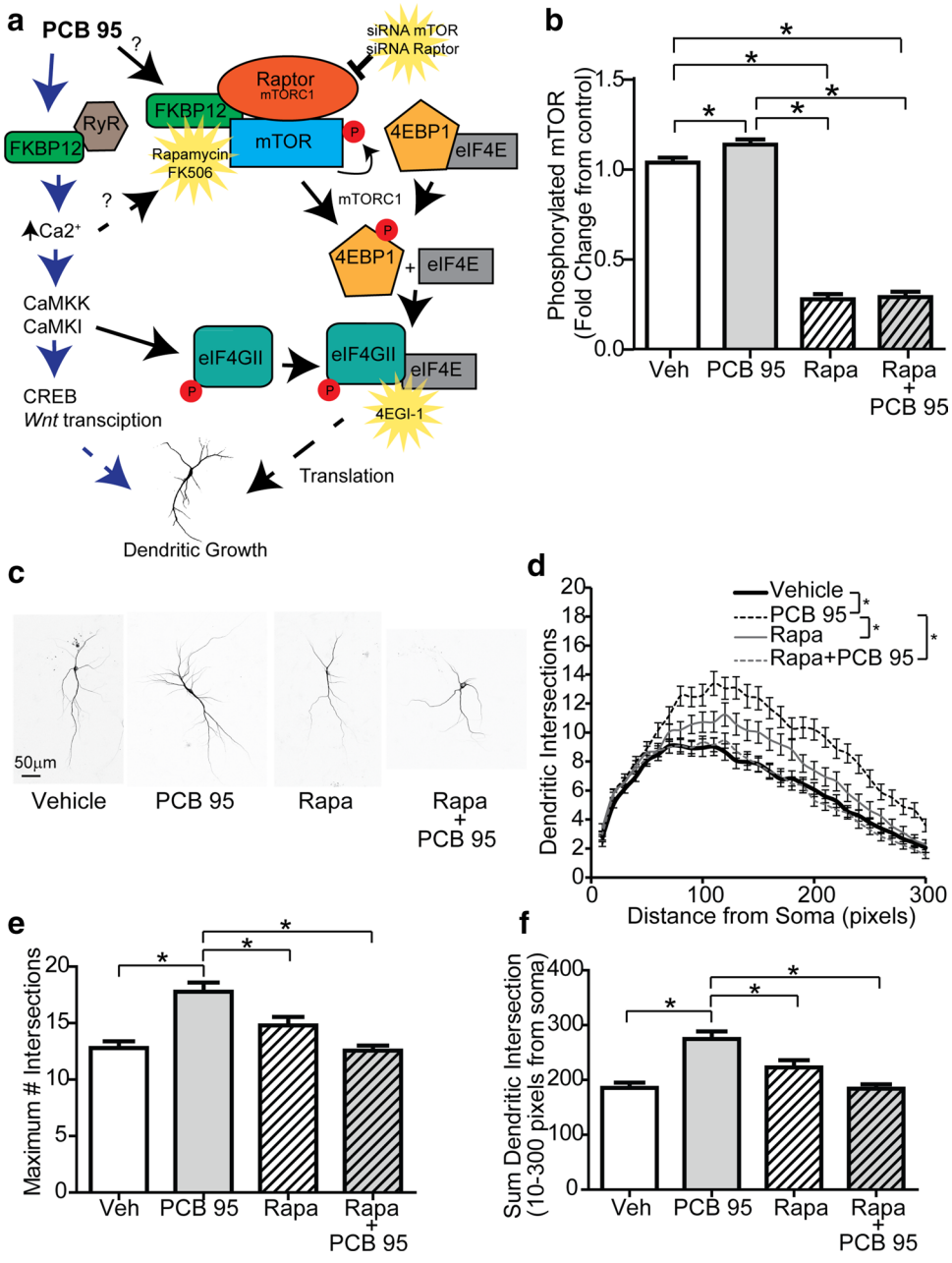

Fig. 2 mTOR signaling is required for PCB 95-induced dendritic growth. **a** Overview of mTOR-mediated mechanisms of activity-dependent dendritic growth. **b** Phosphorylation of mTOR Ser2448 following a 2 h exposure to vehicle (Veh) or PCB 95 (1 nM) in the absence or presence of rapamycin (rapa, 20 nM), as determined by sandwich ELISA. Data presented as mean (±SEM) fold change from vehicle (Veh) control ($n = 4$ independent dissections); differences between groups identified by one-way ANOVA with post hoc Newman-Keuls multiple comparison test. **c** Representative images of 9 DIV neurons expressing MAP2B-EGFP following 48 h exposure to Veh or PCB 95 in the absence of presence of rapa (20 nM). Dendritic growth was quantified by determining: **d** area under the Sholl curve, **e** maximum number of dendritic intersections, and **f** sum of total dendritic intersections. Data presented as mean ± SEM ($n = 79$–82 neurons per group from at least three independent dissections); differences between groups identified using the Kruskal–Wallis test with post hoc Dunn's multiple comparison test. *$p \leq 0.05$

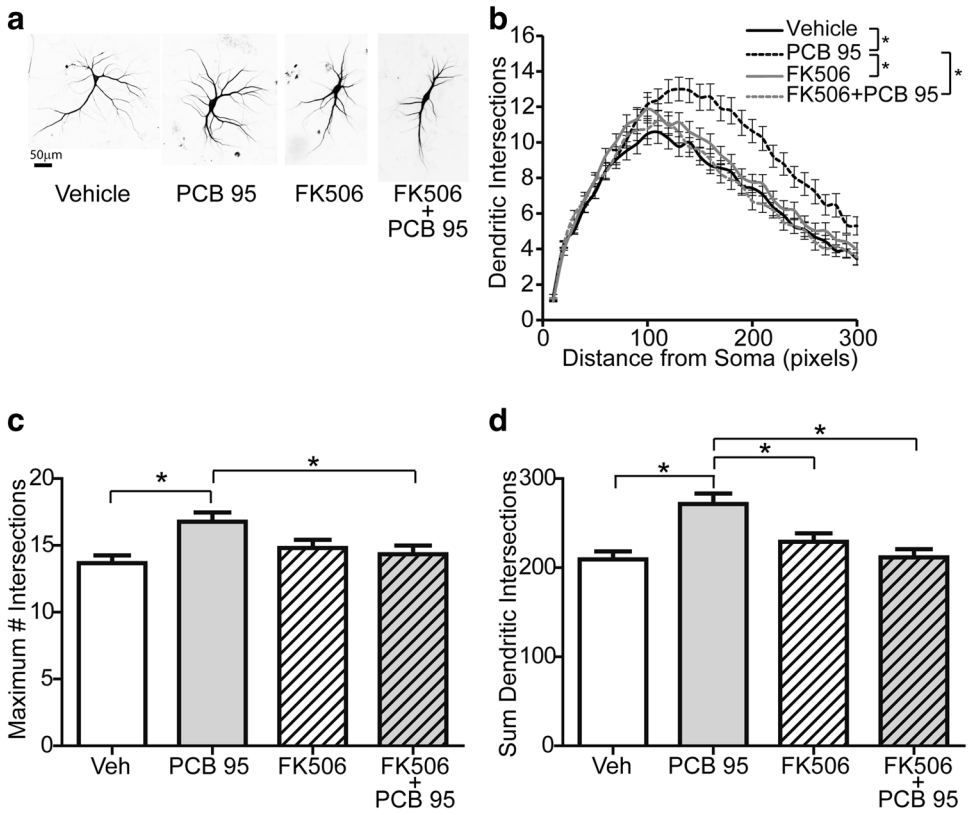

Fig. 3 FK506 blocks PCB 95-induced dendritic growth. **a** Representative images of DIV 9 neurons expressing MAP2B-FusRed following 48 h exposure to vehicle (Veh) or PCB 95 (1 nM) in the absence or presence of FK506 (5 nM). Dendritic complexity quantified as: **b** total area under the Sholl curve; **c** maximum number of dendritic intersections; and **d** sum of total dendritic intersections. Data presented as mean ± SEM ($n = 50–79$ neurons per group from at least two independent dissections); differences between groups identified using the Kruskal–Wallis test with post hoc Dunn's multiple comparison test. *$p \leq 0.05$

siRNA knockdown of mTOR on the dendrite-promoting activity of PCB 95. Transfection with control (scrambled) siRNA did not interfere with the ability of PCB 95 to enhance dendritic growth relative to vehicle control cultures transfected with control siRNA (Fig. 4a, b). In contrast, transfection with mTOR siRNA significantly inhibited PCB 95-induced dendritic growth (Fig. 4c, d). In vehicle control cultures, transfection with mTOR siRNA did not alter dendritic growth compared to cultures transfected with control siRNA (Total AUC, control siRNA 2906 ± 171 vs. mTOR siRNA 3192 ± 120; $p = 0.16$).

Relative roles of mTORC1 vs. mTORC2 in PCB 95-induced dendritic growth

mTOR forms two distinct signaling complexes, mTORC1 and mTORC2, which are in part discriminated by unique partner proteins, raptor and rictor, respectively (Foster and Fingar 2010) and by their sensitivity to rapamycin. Our earlier observation that rapamycin and FK506 blocked PCB 95-induced dendritic growth strongly implicates mTORC1 in mediating PCB 95 effects on dendritic arborization. To confirm that mTOR-dependent translational mechanisms are recruited during PCB 95-induced dendritic growth, we used 4EGI-1, a pharmacologic agent that inhibits eIF4GII from complexing with eIF4E (Fig. 2a), thereby blocking mTORC1-controlled cap-dependent translation without directly affecting the upstream mTOR complex (Huber et al. 2015; Zhou and Huang 2010). Treatment with 4EGI-1 significantly inhibited PCB 95-induced dendritic growth but had no effect on dendritic arborization in vehicle control cultures (Fig. 5).

To test the relative roles of mTORC1 and mTORC2 in PCB 95-induced dendritic arborization, cultures were transfected with siRNA specific for their defining binding partners, raptor and rictor. siRNA knockdown of either raptor or rictor significantly inhibited PCB 95-induced dendritic growth (Fig. 6). Transfection with raptor siRNA also significantly decreased dendritic arborization in vehicle control cultures (Fig. 6). In contrast, blocking mTORC2 by transfection with rictor siRNA caused no significant change in dendritic arborization in vehicle control cultures (Fig. 6).

Discussion

Our results identify a novel mechanism of PCB developmental neurotoxicity in which PCBs promote dendritic growth by activating mTOR signaling. The evidence supporting this model includes: (1) PCB 95 increases mTOR phosphorylation in primary hippocampal cell cultures, and this effect is blocked by rapamycin; and (2) PCB 95-induced dendritic arborization is significantly inhibited by pharmacologic blockade of mTOR or the downstream signaling molecule

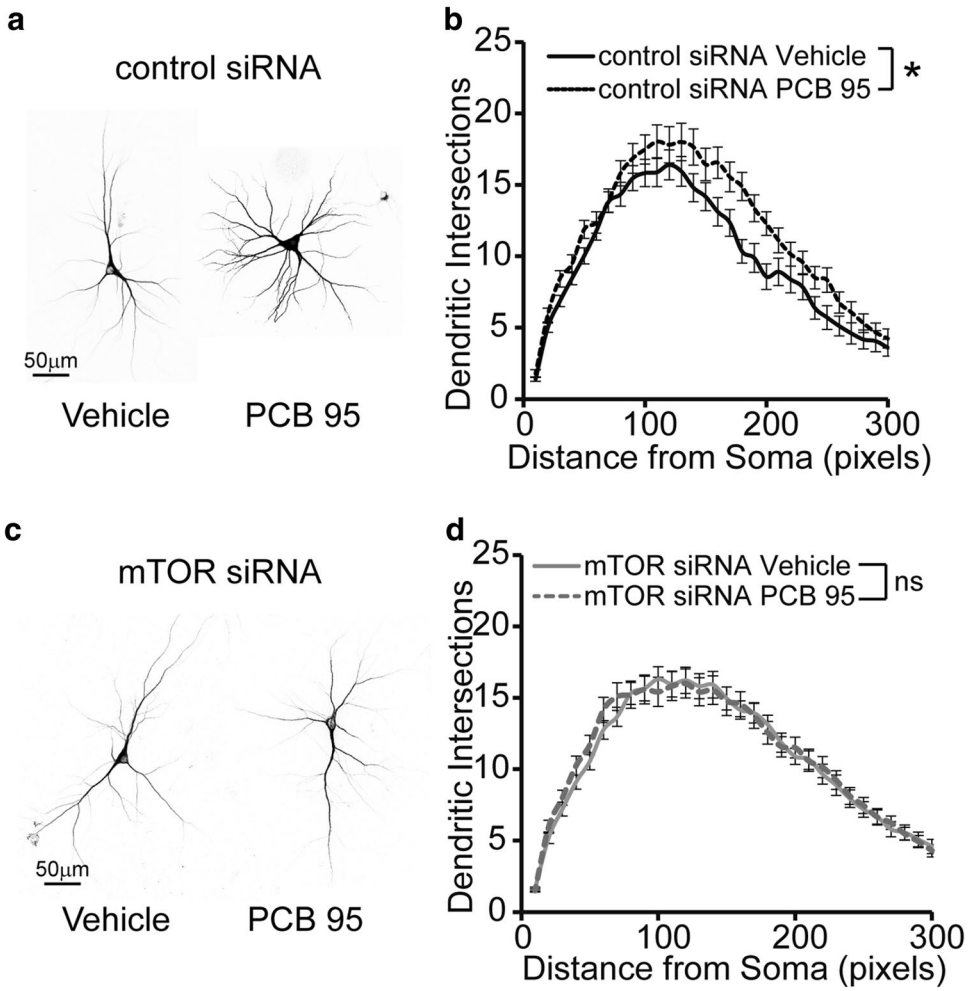

Fig. 4 mTOR siRNA blocks PCB 95-induced dendritic growth. **a, c** Representative images of DIV 9 neurons transfected with MAP2B-FusRed and either control (scrambled) siRNA or mTOR siRNA. **b, d** Dendritic complexity was assessed by quantifying total area under the Sholl curve. Data presented as mean ± SEM ($n = 35$–65 neurons per group from at least three independent dissections); differences between groups identified by the Mann Whitney *U* test. *$p \leq 0.05$; *ns* not significant

4EGI-1, and by siRNA knockdown of mTOR or the mTOR complex proteins, raptor and rictor. These data extend previous reports of PCB effects on mTOR signaling in hepatic cell lines (Hardesty et al. 2017; Shi et al. 2016), although in these studies Aroclor 1260 and a quinone metabolite of PCB 29 were observed to inhibit mTOR signaling. The reason(s) for the discrepant effects of PCBs on mTOR are not known but likely reflect differences with respect to the model systems (primary neurons vs. hepatic cell lines) and/or the PCB congeners investigated. However, our findings are consistent with recent observations that Atlantic killifish exposed to high PCB levels in the New Bedford Harbor express elevated levels of mTOR compared to Atlantic killifish from cleaner waters (Fritsch et al. 2015).

A key question raised by these studies is how PCB 95 activates mTOR. Our immunocytochemical analyses of primary hippocampal neurons indicating that RyRs are in close physical proximity to mTOR and FKBP12, suggest a model in which PCB 95 sensitization of neuronal RyRs increases local concentrations of intracellular Ca^{2+} ($[Ca^{2+}]_i$), which then activate mTOR (Fig. 2a). In support of this model, PCB 95 has potent RyR activity (Holland et al. 2017), directly binding to and stabilizing these Ca^{2+} ion channels in their open configuration (Pessah et al. 2010), and PCB 95-RyR interactions have been causally linked to increased $[Ca^{2+}]_i$ in primary hippocampal neurons (Wayman et al. 2012a). In further support of this model, several lines of evidence demonstrate that mTOR is activated by increased $[Ca^{2+}]_i$: (i) Ca^{2+} is required for mTORC1 signaling (Gulati et al. 2008) and (ii) calmodulin binds mTORC1 to activate its kinase activity in a Ca^{2+}-dependent manner (Li et al. 2016). Collectively, these observations support a model in which PCB 95 activates mTORC1 via Ca^{2+}-dependent mechanisms downstream of RyR sensitization.

Alternatively, PCB 95 may promote mTOR signaling via interactions with the immunophilin, FKBP12 (Fig. 2a). FKBP12 is a functional component of mTORC1 (Zhou

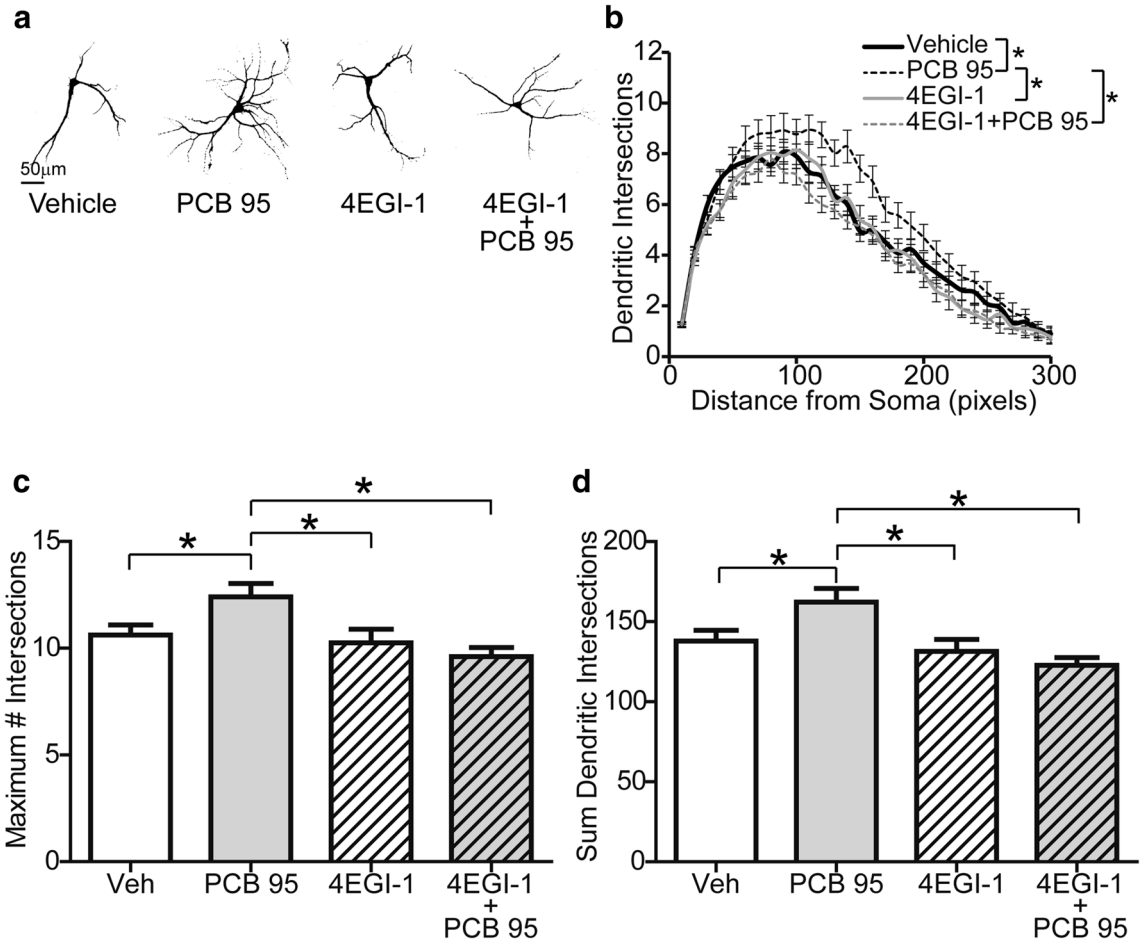

Fig. 5 Pharmacological block of eIF4GII and eIF4E complex formation with 4EGI-1 inhibits PCB 95-induced dendritic growth. **a** Representative images of DIV 9 neurons transfected with MAP2B-FusRed following 48 h exposure to vehicle (Veh) or PCB 95 (1 nM) in the absence or presence of 4EGI-1 (1 μM). Dendritic complexity was assessed by quantifying: **b** total area under the Sholl curve; **c** maximum number of dendritic intersections; and **d** sum of total dendritic intersections. Data presented as mean ± SEM ($n = 27$–41 neurons per group from at least two independent dissections); differences between groups identified by one-way ANOVA with post hoc Newman–Keuls multiple comparison test. *$p \leq 0.05$

and Huang 2010), and FKBP12 is also required for PCB 95 sensitization of RyRs (Pessah et al. 2010). Rapamycin and FK506 block mTOR signaling by binding to FKBP12 to alter its activity (Ballou and Lin 2008; Sarbassov et al. 2006), and we observed that these pharmacologic agents blocked PCB 95 effects on mTOR activation and dendritic arborization in hippocampal neurons. One interpretation of these data is that rapamycin and FK506 block RyR sensitization by PCB 95, thereby preventing Ca^{2+}-dependent activation of mTOR; the alternative interpretation is that PCB 95 interacts directly with mTORC complexes via FKBP12. Distinguishing between these possibilities is the focus of future studies.

Results from our studies of the relative roles of mTORC1 and mTORC2 in dendritic growth were surprising. These mTORC complexes are differentiated by their sensitivity to rapamycin, with mTORC1 being sensitive, while mTORC2 is relatively insensitive (Sarbassov et al. 2006), as well as their interaction with FKBP12, which is unique to mTORC1 (Marz et al. 2013). Because both rapamycin and FK506 blocked PCB 95-induced dendritic growth, we anticipated that siRNA knockdown of raptor, but not rictor, would significantly inhibit the dendrite-promoting activity of PCB 95. However, we observed that siRNA knockdown of either raptor or rictor blocked PCB 95-induced dendritic growth. Two interpretations of these data are: (i) activity of both mTORC1 and mTORC2 are required for PCB effects on dendritic growth, perhaps with mTORC2 activating mTORC1 via AKT signaling (Switon et al. 2017); and/or (ii) rapamycin and FK506 effects on PCB 95-induced dendritic growth are mediated at the level of the RyR.

Another unexpected outcome was that inhibition of mTORC1 with raptor siRNA knockdown decreased dendritic complexity in vehicle control cultures, whereas

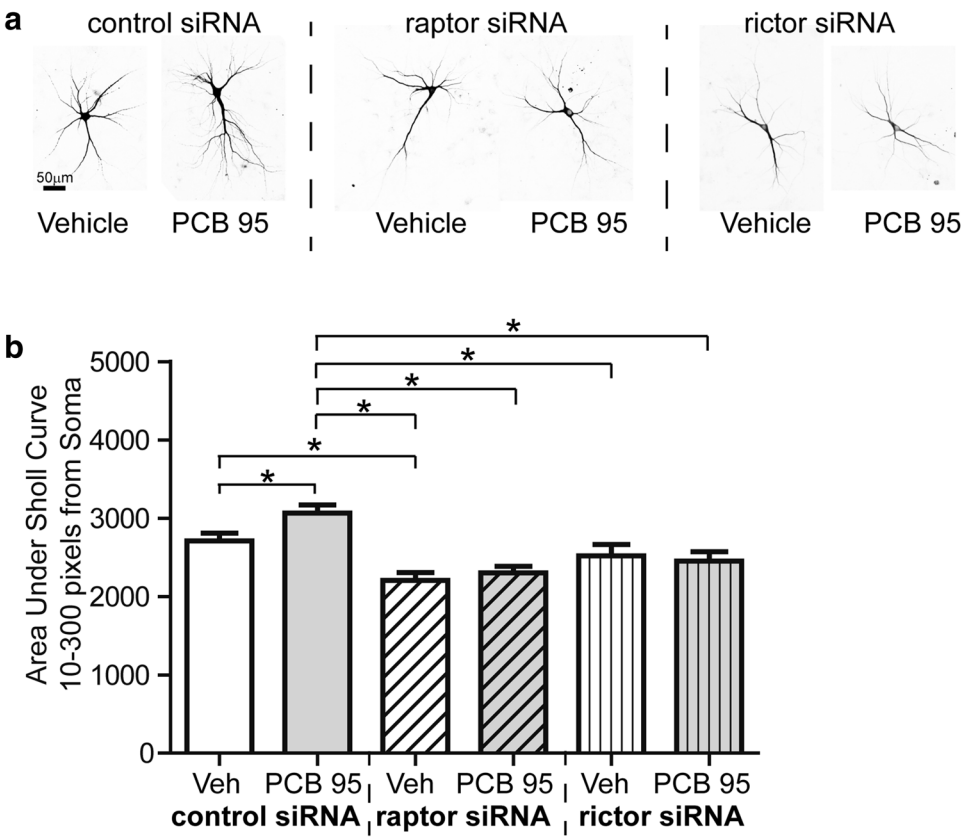

Fig. 6 PCB 95-induced dendritic growth requires both mTORC1 and mTORC2. **a** Representative images of DIV 9 neurons transfected with MAP2B-EGFP and either control (scrambled) siRNA, raptor siRNA (mTORC1), or rictor siRNA (mTORC2) following 48 h exposure to vehicle (Veh) or PCB 95 (1 nM). **b** Dendritic complexity was assessed by quantifying total area under the Sholl curve. Data presented as mean ± SEM ($n = 43$–97 neurons per group from at least two independent dissections). Differences between groups identified by one-way ANOVA with post hoc Newman–Keuls multiple comparison test. *$p \leq 0.05$

inhibition of mTORC2 with rictor siRNA knockdown had no effect in the absence of PCB 95. This suggests that basal dendritic arborization may rely more on mTORC1 than mTORC2 signaling. In support of this, targeted deletion of raptor in the brain severely reduces neural cell number, size, and differentiation and results in early postnatal death (Cloetta et al. 2013), whereas targeted deletion of rictor in the brain causes non-lethal microcephaly (Angliker et al. 2015; Thomanetz et al. 2013). Similarly, comparative studies of mice with targeted deletion of either raptor or rictor in Purkinje cells revealed more pronounced effects of mTORC1 on Purkinje cell soma size, electrophysiology, cell survival and behavior (Angliker 2015). However, both genotypes increased dendritic arborization of Purkinje cells (Angliker et al. 2015). Similarly, both mTORC1 and mTORC2 signaling promote dendritic growth in olfactory bulb neurons (Skalecka et al. 2016) and hippocampal neurons (Urbanska et al. 2012). Consistent with these observations, inhibition of either mTORC1 or mTORC2 activity by siRNA knockdown of raptor or rictor, respectively, blocked the dendrite promoting activity of PCB 95.

Dendritic morphology is a major determinant of neuronal connectivity that is often perturbed in NDDs, and genes important for regulating dendritic shape and size during development have been identified as genetic risk factors in many NDDs (Copf 2016; Ebert and Greenberg 2013; Penzes et al. 2011; Stamou et al. 2013). Because of its well-established role in regulating dendritic growth and synaptic density (Urbanska et al. 2012), it is not surprising that mTOR signaling has been implicated in the pathogenesis of several NDDs (Gipson and Johnston 2012; Wang and Doering 2013). Collectively, these published data, together with the findings of this study, identify mTOR signaling as a convergence point for gene by environment interactions that confer risk for adverse neurodevelopmental outcomes. In support of this, increasing experimental and epidemiological evidence link environmental PCBs to elevated risk for NDDs (Korrick and Sagiv 2008; Lyall et al. 2017b; Stamou et al. 2013), and PCB 95 levels are higher in post-mortem brain tissue of children diagnosed with a syndromic form of autism relative to neurotypical controls (Mitchell et al. 2012). This, together with the known role of PCB 95 in inducing dendritic growth in rodent models both in vivo and in vitro (Wayman et al. 2012a, b; Yang et al. 2009), suggest that PCB 95, and potentially other RyR-active environmental chemicals, interact with mutations in the mTOR signaling pathway to alter dendritic complexity and increase NDD risk.

Acknowledgements This research was supported by the National Institute of Environmental Health Sciences (Grants ES014901, ES011269, and ES023513) and the United States Environmental Protection Agency (Grant R833292). KPK was supported by a postdoctoral fellowship from the National Institute of Child Health and

Human Development (F32 HD088016); GWM, by a postdoctoral fellowship from the National Institute of Environmental Health Sciences (F32 ES024070); and SS and HC by predoctoral fellowships from the National Institute of Environmental Health Sciences (T32 ES007059). This research used the Biological Analysis Core of the UC Davis MIND Institute Intellectual and Developmental Disabilities Research Center (U54 HD079125). We also acknowledge support provided by Michael Paddy, Director of the Molecular and Cell Biology Light Microscope Imaging Facility (UC Davis CRCF Core Facility) for use of the Nikon SIM (acquired via NIH Grant 1 S10 RR029304-0). The funding agencies were not involved in experimental design, data analysis or decision to publish, and the content is solely the responsibility of the authors and does not necessarily represent the official views of the funding agencies. Furthermore, the funding agencies do not endorse the purchase of any commercial products or services mentioned in the publication.

Compliance with ethical standards

Conflict of interest The authors declare that they have no conflict of interest.

Ethical approval All applicable international, national, and/or institutional guidelines for the care and use of animals were followed. The manuscript does not contain clinical studies or patient data.

References

Angliker N, Burri M, Zaichuk M, Fritschy JM, Ruegg MA (2015) mTORC1 and mTORC2 have largely distinct functions in Purkinje cells. Eur J Neurosci 42(8):2595–2612. https://doi.org/10.1111/ejn.13051

Ballou LM, Lin RZ (2008) Rapamycin and mTOR kinase inhibitors. J Chem Biol 1(1–4):27–36. https://doi.org/10.1007/s12154-008-0003-5

Berghuis SA, Bos AF, Sauer PJ, Roze E (2015) Developmental neurotoxicity of persistent organic pollutants: an update on childhood outcome. Arch Toxicol 89(5):687–709. https://doi.org/10.1007/s00204-015-1463-3

Chen H, Streifel KM, Singh V et al (2017) From the cover: BDE-47 and BDE-49 inhibit axonal growth in primary rat hippocampal neuron-glia co-cultures via ryanodine receptor-dependent mechanisms. Toxicol Sci 156(2):375–386. https://doi.org/10.1093/toxsci/kfw259

Cloetta D, Thomanetz V, Baranek C et al (2013) Inactivation of mTORC1 in the developing brain causes microcephaly and affects gliogenesis. J Neurosci 33(18):7799–7810. https://doi.org/10.1523/JNEUROSCI.3294-12.2013

Copf T (2016) Impairments in dendrite morphogenesis as etiology for neurodevelopmental disorders and implications for therapeutic treatments. Neurosci Biobehav Rev 68:946–978. https://doi.org/10.1016/j.neubiorev.2016.04.008

Ebert DH, Greenberg ME (2013) Activity-dependent neuronal signalling and autism spectrum disorder. Nature 493(7432):327–337. https://doi.org/10.1038/nature11860

Ferreira TA, Blackman AV, Oyrer J et al (2014) Neuronal morphometry directly from bitmap images. Nat Methods 11(10):982–984. https://doi.org/10.1038/nmeth.3125

Foster KG, Fingar DC (2010) Mammalian target of rapamycin (mTOR): conducting the cellular signaling symphony. J Biol Chem 285(19):14071–14077. https://doi.org/10.1074/jbc.R109.094003

Fritsch EB, Stegeman JJ, Goldstone JV et al (2015) Expression and function of ryanodine receptor related pathways in PCB tolerant Atlantic killifish (*Fundulus heteroclitus*) from New Bedford Harbor, MA, USA. Aquat Toxicol 159:156–166. https://doi.org/10.1016/j.aquatox.2014.12.017

Gipson TT, Johnston MV (2012) Plasticity and mTOR: towards restoration of impaired synaptic plasticity in mTOR-related neurogenetic disorders. Neural Plast 2012:486402. https://doi.org/10.1155/2012/486402

Gulati P, Gaspers LD, Dann SG et al (2008) Amino acids activate mTOR complex 1 via Ca2+/CaM signaling to hVps34. Cell Metab 7(5):456–465. https://doi.org/10.1016/j.cmet.2008.03.002

Gustafsson MG, Shao L, Carlton PM et al (2008) Three-dimensional resolution doubling in wide-field fluorescence microscopy by structured illumination. Biophys J 94(12):4957–4970. https://doi.org/10.1529/biophysj.107.120345

Hardesty JE, Wahlang B, Falkner KC et al (2017) Polychlorinated biphenyls disrupt hepatic epidermal growth factor receptor signaling. Xenobiotica 47(9):807–820. https://doi.org/10.1080/00498254.2016.1217572

Herrick RF, Lefkowitz DJ, Weymouth GA (2007) Soil contamination from PCB-containing buildings. Environ Health Perspect 115(2):173–175. https://doi.org/10.1289/ehp.9646

Heyer DB, Meredith RM (2017) Environmental toxicology: sensitive periods of development and neurodevelopmental disorders. Neurotoxicology 58:23–41. https://doi.org/10.1016/j.neuro.2016.10.017

Holland EB, Feng W, Zheng J et al (2017) An extended structure-activity relationship of nondioxin-like PCBs evaluates and supports modeling predictions and identifies picomolar potency of PCB 202 towards ryanodine receptors. Toxicol Sci 155(1):170–181. https://doi.org/10.1093/toxsci/kfw189

Huber KM, Klann E, Costa-Mattioli M, Zukin RS (2015) Dysregulation of *Mammalian* target of rapamycin signaling in mouse models of autism. J Neurosci 35(41):13836–13842. https://doi.org/10.1523/JNEUROSCI.2656-15.2015

Keil KP, Sethi S, Wilson MD, Chen H, Lein PJ (2017) In vivo and in vitro sex differences in the dendritic morphology of developing murine hippocampal and cortical neurons. Sci Rep 7(1):8486. https://doi.org/10.1038/s41598-017-08459-z

Kindler S, Kreienkamp HJ (2012) Dendritic mRNA targeting and translation. Adv Exp Med Biol 970:285–305. https://doi.org/10.1007/978-3-7091-0932-8_13

Koh WX, Hornbuckle KC, Wang K, Thorne PS (2016) Serum polychlorinated biphenyls and their hydroxylated metabolites are associated with demographic and behavioral factors in children and mothers. Environ Int 94:538–545. https://doi.org/10.1016/j.envint.2016.06.014

Korrick SA, Sagiv SK (2008) Polychlorinated biphenyls, organochlorine pesticides and neurodevelopment. Curr Opin Pediatr 20(2):198–204. https://doi.org/10.1097/MOP.0b013e3282f6a4e9

Landrigan PJ, Lambertini L, Birnbaum LS (2012) A research strategy to discover the environmental causes of autism and neurodevelopmental disabilities. Environ Health Perspect 120(7):a258–60. https://doi.org/10.1289/ehp.1104285

Lesiak A, Zhu M, Chen H et al (2014) The environmental neurotoxicant PCB 95 promotes synaptogenesis via ryanodine receptor-dependent miR132 upregulation. J Neurosci 34(3):717–725. https://doi.org/10.1523/JNEUROSCI.2884-13.2014

Li RJ, Xu J, Fu C et al (2016) Regulation of mTORC1 by lysosomal calcium and calmodulin. Elife https://doi.org/10.7554/eLife.19360

Lyall K, Croen L, Daniels J et al (2017a) The changing epidemiology of autism spectrum disorders. Annu Rev Public Health 38:81–102. https://doi.org/10.1146/annurev-publhealth-031816-044318

Lyall K, Croen LA, Sjodin A et al (2017b) Polychlorinated biphenyl and organochlorine pesticide concentrations in maternal mid-pregnancy serum samples: association with autism spectrum disorder and intellectual disability. Environ Health Perspect 125(3):474–480. https://doi.org/10.1289/EHP277

Marek RF, Thorne PS, Herkert NJ, Awad AM, Hornbuckle KC (2017) Airborne PCBs and OH-PCBs inside and outside urban and rural US schools. Environ Sci Technol 51(14):7853–7860. https://doi.org/10.1021/acs.est.7b01910

Marz AM, Fabian AK, Kozany C, Bracher A, Hausch F (2013) Large FK506-binding proteins shape the pharmacology of rapamycin. Mol Cell Biol 33(7):1357–1367. https://doi.org/10.1128/MCB.00678-12

Mitchell MM, Woods R, Chi LH et al (2012) Levels of select PCB and PBDE congeners in human postmortem brain reveal possible environmental involvement in 15q11-q13 duplication autism spectrum disorder. Environ Mol Mutagen 53(8):589–598. https://doi.org/10.1002/em.21722

Penzes P, Cahill ME, Jones KA, VanLeeuwen JE, Woolfrey KM (2011) Dendritic spine pathology in neuropsychiatric disorders. Nat Neurosci 14(3):285–293. https://doi.org/10.1038/nn.2741

Pessah IN, Cherednichenko G, Lein PJ (2010) Minding the calcium store: ryanodine receptor activation as a convergent mechanism of PCB toxicity. Pharmacol Ther 125(2):260–285. https://doi.org/10.1016/j.pharmthera.2009.10.009

Sable HJK, Schantz SL (2006) Executive function following developmental exposure to polychlorinated biphenyls (PCBs): what animal models have told US. In: Levin ED, Buccafusco JJ (eds) Animal models of cognitive impairment. Frontiers in Neuroscience, Boca Raton

Sarbassov DD, Ali SM, Sengupta S et al (2006) Prolonged rapamycin treatment inhibits mTORC2 assembly and Akt/PKB. Mol Cell 22(2):159–168. https://doi.org/10.1016/j.molcel.2006.03.029

Schindelin J, Arganda-Carreras I, Frise E et al (2012) Fiji: an open-source platform for biological-image analysis. Nat Methods 9(7):676–682. https://doi.org/10.1038/nmeth.2019

Schneider CA, Rasband WS, Eliceiri KW (2012) NIH Image to ImageJ: 25 years of image analysis. Nat Methods 9(7):671–675

Schreiber KH, Ortiz D, Academia EC, Anies AC, Liao CY, Kennedy BK (2015) Rapamycin-mediated mTORC2 inhibition is determined by the relative expression of FK506-binding proteins. Aging Cell 14(2):265–273. https://doi.org/10.1111/acel.12313

Shi Q, Song X, Liu Z et al (2016) Quinones derived from polychlorinated biphenyls induce ROS-dependent autophagy by evoking an autophagic flux and inhibition of mTOR/p70S6k. Chem Res Toxicol 29(7):1160–1171. https://doi.org/10.1021/acs.chemrestox.6b00127

Skalecka A, Liszewska E, Bilinski R et al (2016) mTOR kinase is needed for the development and stabilization of dendritic arbors in newly born olfactory bulb neurons. Dev Neurobiol 76(12):1308–1327. https://doi.org/10.1002/dneu.22392

Sosanya NM, Cacheaux LP, Workman ER, Niere F, Perrone-Bizzozero NI, Raab-Graham KF (2015) Mammalian target of rapamycin (mTOR) tagging promotes dendritic branch variability through the capture of Ca2+/calmodulin-dependent protein kinase II alpha (CaMKIIalpha) mRNAs by the RNA-binding protein HuD. J Biol Chem 290(26):16357–16371. https://doi.org/10.1074/jbc.M114.599399

Stamou M, Streifel KM, Goines PE, Lein PJ (2013) Neuronal connectivity as a convergent target of gene x environment interactions that confer risk for autism spectrum disorders. Neurotoxicol Teratol 36:3–16. https://doi.org/10.1016/j.ntt.2012.12.001

Switon K, Kotulska K, Janusz-Kaminska A, Zmorzynska J, Jaworski J (2017) Molecular neurobiology of mTOR. Neuroscience 341:112–153. https://doi.org/10.1016/j.neuroscience.2016.11.017

Thomanetz V, Angliker N, Cloetta D et al (2013) Ablation of the mTORC2 component rictor in brain or Purkinje cells affects size and neuron morphology. J Cell Biol 201(2):293–308. https://doi.org/10.1083/jcb.201205030

Troca-Marin JA, Alves-Sampaio A, Montesinos ML (2012) Deregulated mTOR-mediated translation in intellectual disability. Prog Neurobiol 96(2):268–282. https://doi.org/10.1016/j.pneurobio.2012.01.005

Ulbrich B, Stahlmann R (2004) Developmental toxicity of polychlorinated biphenyls (PCBs): a systematic review of experimental data. Arch Toxicol 78(5):252–268. https://doi.org/10.1007/s00204-003-0519-y

Urbanska M, Gozdz A, Swiech LJ, Jaworski J (2012) Mammalian target of rapamycin complex 1 (mTORC1) and 2 (mTORC2) control the dendritic arbor morphology of hippocampal neurons. J Biol Chem 287(36):30240–30256. https://doi.org/10.1074/jbc.M112.374405

Wang H, Doering LC (2013) Reversing autism by targeting downstream mTOR signaling. Front Cell Neurosci 7:28. https://doi.org/10.3389/fncel.2013.00028

Wayman GA, Impey S, Marks D et al (2006) Activity-dependent dendritic arborization mediated by CaM-kinase I activation and enhanced CREB-dependent transcription of Wnt-2. Neuron 50(6):897–909. https://doi.org/10.1016/j.neuron.2006.05.008

Wayman GA, Bose DD, Yang D et al (2012a) PCB-95 modulates the calcium-dependent signaling pathway responsible for activity-dependent dendritic growth. Environ Health Perspect 120(7):1003–1009. https://doi.org/10.1289/ehp.1104833

Wayman GA, Yang D, Bose DD et al (2012b) PCB-95 promotes dendritic growth via ryanodine receptor-dependent mechanisms. Environ Health Perspect 120(7):997–1002. https://doi.org/10.1289/ehp.1104832

Yang D, Kim KH, Phimister A et al (2009) Developmental exposure to polychlorinated biphenyls interferes with experience-dependent dendritic plasticity and ryanodine receptor expression in weanling rats. Environ Health Perspect 117(3):426–435. https://doi.org/10.1289/ehp.11771

Zhou H, Huang S (2010) The complexes of mammalian target of rapamycin. Curr Protein Pept Sci 11(6):409–424